Hindawi
International Journal of Photoenergy
Volume 2021, Article ID 1508469, 9 pages
https://doi.org/10.1155/2021/1508469

Research Article

Impact on Structural and Optical Properties of CZTS Thin Films with Solvents and Ge Incorporation

Abhay Kumar Singh,[1,2,3] **Tanka R. Rana**,[3] **JunHo Kim**,[3] **M. Shkir**,[4] **and Tien-Chien Jen**[1]

[1]*Department of Mechanical Engineering Science, University of Johannesburg, South Africa*
[2]*Department of Electronics Engineering, Incheon National University, Incheon 406-772, Republic of Korea*
[3]*Department of Physics, Incheon National University, Incheon 406-772, Republic of Korea*
[4]*Advanced Functional Materials and Optoelectronics Laboratory (AFMOL), Department of Physics, Faculty of Science, King Khalid University, P.O. Box 9004, Abha, Saudi Arabia*

Correspondence should be addressed to Abhay Kumar Singh; abhaysngh@rediffmail.com

Received 31 December 2019; Revised 15 February 2020; Accepted 28 March 2020; Published 18 March 2021

Academic Editor: Leonardo Palmisano

This report demonstrates nontoxic colloidal nitrate route CZTS (Cu_2ZnSnS_4) synthesis at room temperature, along with their band grading due to incorporation of Ge as cost of Sn (3%). The parent CZTS, CZGTS ($Cu_2ZnGeSnS_4$), and their polyvinyl alcohol (PVA), dimethyl sulfoxide (DMSO) solvent containing solutions doctor blade-coated thin film structural and optical properties are discussed. Their sulfurized thin films thickness have been achieved $\pm 2\,\mu$. It has noticed that addition of Ge in CZTS alloy affects the grain sizes, crystallographic structure, Raman spectral peak shift toward the higher wave number side. The addition of PVA and DMSO is also substantially contributed in their physical property modification by demonstrating the gradual improvement in grain sizes and compactness. Moreover, the gradual changes have also appeared in their X-ray diffractometer (XRD) and Raman spectroscopic results. The optical energy band gaps of the CZTS, CZGTS, and their PVA, DMSO mixed alloyed thin films are obtained in between 1.27 eV to 1.57 eV and 1.58 eV to 1.83 eV.

1. Introduction

With the increasing consumption of conventional energy with the gradual serious environmental problems worldwide, the researchers have paid much attention toward research and application of solar cells [1, 2], to fulfill the next-generation worldwide power consumption requirements upto terawatt (TW) level. This can be achieved only considering a few key issues, like photovoltaic materials should be cost-effective, earth abundant, offer a long functional lifetime, and have high power conversion efficiency with the direct energy gap [1–3]. Considering these key factors in the recent years, investigators have been recognized inorganic (chalcogen) multilayer photovoltaic (PV) technologies can reduce production cost in terms of both raw materials and processing requirements [1–3]. Therefore, in the running decade, thin film preparation technologies have been widely promoted from the innovations considering the noticeable advantages: less material requirement, easy to deposit on different (glass, stainless steel, and plastic) kinds of the flexible substrates, and overall device cost reduction.

More than a decade quaternary Cu_2ZnSnS_4 (CZTS) absorber has drawn tremendous attention to make solar devices. Its suitable direct energy band gap (~1.5 eV), high absorption coefficient ($\sim 10^5\,cm^{-1}$) with nontoxicity, and abundant availability of the elements in the earth crust make them favorable for the photovoltaic technology. Additionally, prospective CZTS can also have performance advantages in comparison with counterpart materials like CdTe and CIGS (CuInGaSe) [4, 5]. The direct liquid deposition approaches are particularly attractive for large-scale manufacturing due to their compatibility with large-scale deposition techniques such as tape casting. Several investigators have been demonstrated the fabrication of CZTS solar cells using a variety of

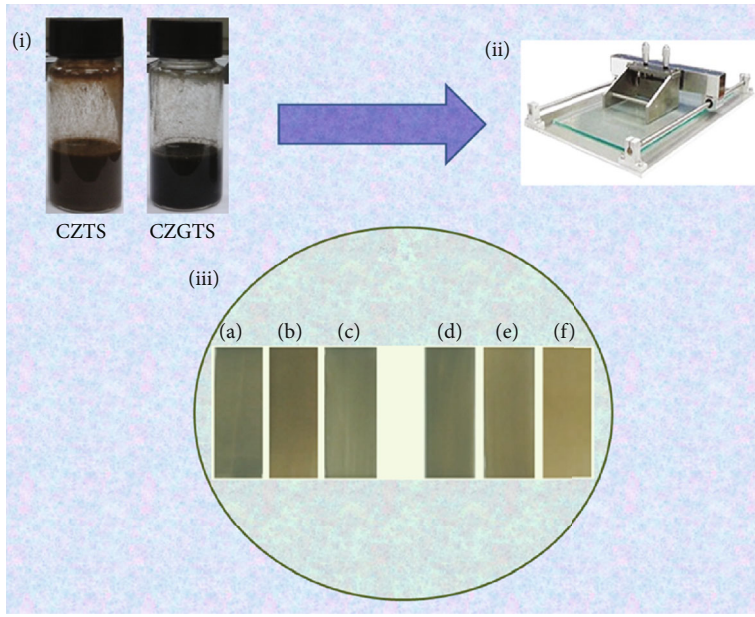

Figure 1: (i) CZTS and CZGTS synthesized solutions; (ii) used doctor blade coater; (iii) (a, b, c). CZTS, CZTS-PVA, and CZTS-DMSO doctor blade-coated sulfurized thin films on SLG soda lime glass substrate; (d, e, f) CZGTS, CZGTS-PVA, and CZGTS-DMSO, doctor blade-coated sulfurized thin films on SLG soda lime glass substrate.

methods including spray pyrolysis, evaporation, sputtering, sol-gel processing, electrodeposition, and nanocrystal synthesis [6, 7]. Typically, colloidal route cell fabrication involves oleylamine and chlorides employing certain temperature range; therefore, formed defects act as a hole/recombination centers during the photovoltaic conversion. Despite the adequate high-performance crystallinity, such routes synthesized materials having hazardous toxicity issue [8]. Considering numerous drawback issues of the existing CZTS processing, researchers have paid attention to synthesized non (or less) hazardous solution by selecting suitable CZT nitrate compounds with the host sulfur [8–10].

Despite the tremendous possibility of the kesterite CZTS, it is a mirror fact that their efficiency has not been achieved beyond ~10%; however, from the theoretical predictions, it can be upto 32.2% [11–13]. To get high efficiency in CZTS-based devices, investigators are making efforts by varying material compositions, preparation methods, etc. [1]. An approach CZTS band grading from the element germanium (Ge) is also getting much attention. It has predicted that CZTS alloying with Ge can provide a suitable band grading in CZTS; therefore, overall active layer working performance may improve [14–16]. Thus, one technique can lead the band gap engineering for the CZTS by the partial replacement of element tin (Sn) from Ge [15]. Among this, performance of solar cell devices is also depending on active layer thin film quality and grain sizes. Therefore, under the nonvacuum thin film preparation used, solution binder can also play a crucial role [14, 15].

Considering above discussed key issues, the CZTS solar cell active layer material property investigations predominately have been devoted to different deposition process. A few reports are available on CZTS absorber layer along with element Ge band grading, toxicity, and impact of the different solution binders. Therefore, determination of such casual physical properties of CZTS absorber layer material is an important matter [14–16]. Hence, this study deals CZTS absorber layer band grading from the semimetallic element Ge by replacing the amount of the Sn, with the nontoxic nitrate parent solution as well as PVA (polyvinyl alcohol) and DMSO (dimethyl sulfoxide) mixed solutions.

2. Experimental Procedure

To make a colloidal solution of CZTS and CZGTS materials, the appropriate compositions were taken in the ratio: Cu = 22.05, Zn = 13.5, Sn = 11, and S = 53.45 and Cu = 22.05, Zn = 13.5, Ge = 3, Sn = 9, and S = 53.45. The required materials copper nitratehydrate ($Cu(NO_3)_2$ $3H_2O$), zinc nitratehydrate ($Zn(NO_3)_2$ $6H_2O$), pure tin (Sn) (99.999%) powder, sulfur (S), and germanium (Ge) (99.999%) powder were purchased from the sigma Aldrich. Three separate solutions A, B, and C were made to dissolve cations and anions. Solution A contained $Cu(NO_3)_2$ $3H_2O$ (5 m mole), Thiourea (CH_4N_2S) (10 g), and 5 ml DI water for both CZTS and CZGTS compositions. Solution B was made by taking $Zn(NO_3)_2$ $6H_2O$ (5 m mole) and 6 ml ammonia (NH_4OH) water for both CZTS and CZGTS compositions. Solution C was made from addition of the tin (Sn) (5 m mole), sulfur (10 m mole), and aqueous ammonium sulfide solution ($(NH_4)_2S$) for the CZTS, while in the case of CZGTS, amount of Ge powder was added into the solution. To dissolve Cu cations and anions in solutions A and C, initial stirrer was pursued. Afterward, appropriate amount of the water content was added in solutions A, B, and C. Then, solutions A and C were kept for the 2-3 h stirring under the normal atmospheric environment. In the subsequent process, solutions A, B, and C were mixed together to make CZTS and CZGTS complex compositions.

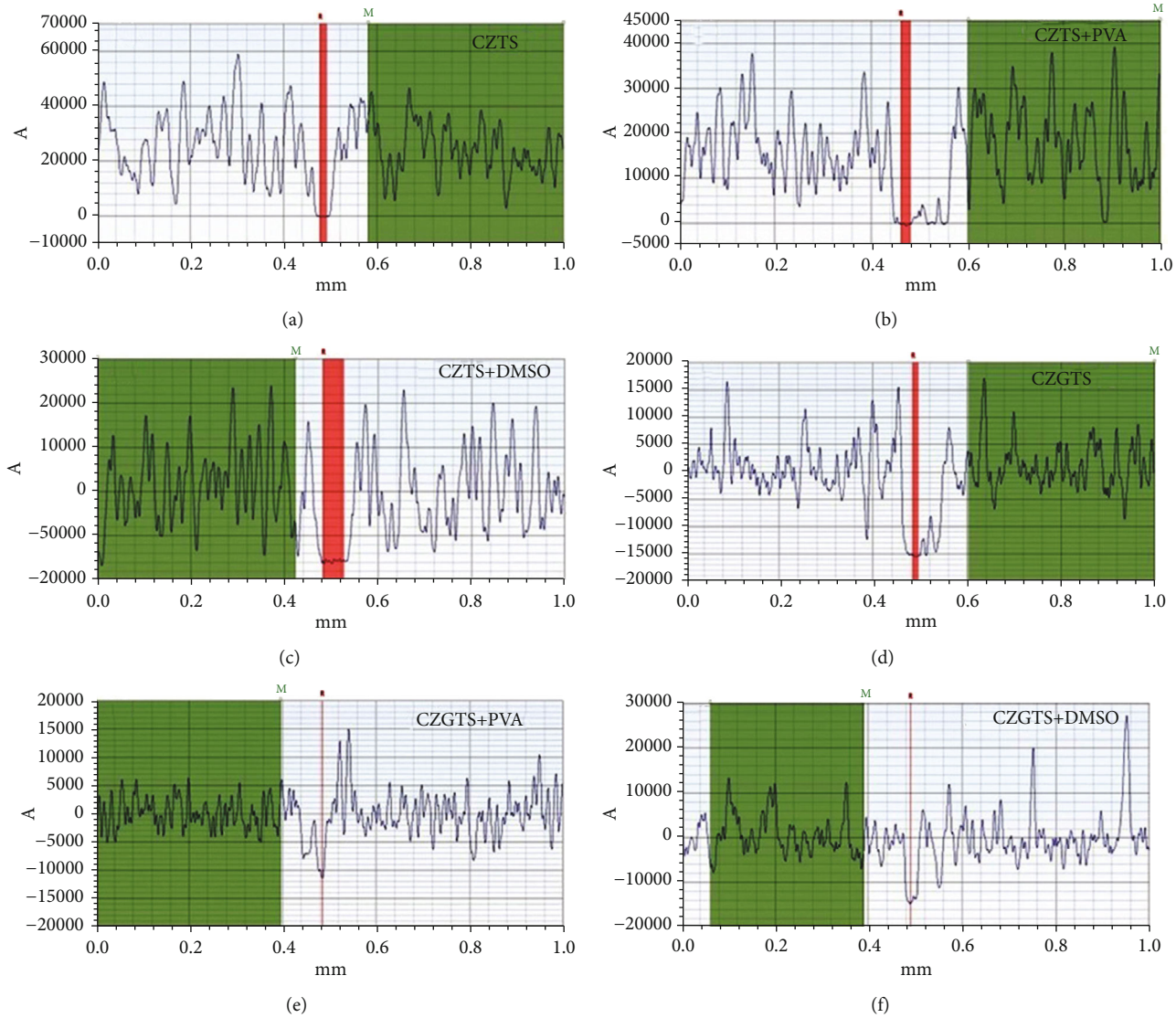

Figure 2: (a–c) CZTS, CZTS-PVA, and CZTS-DMSO; (d–f) CZGTS, CZGTS-PVA, and CZGTS-DMSO thickness profillometer results.

In the beginning, CZTS and CZGTS solution colour was dark reddish; however, with the continuous vigorous stirring at 60°C ± 10, their colour transformed into dark black. The formed CZTS and CZGTS crystals/particles were separated from the complex solution after allowing 12 h decantation process at normal room temperature. The separated part of the CZTS and CZGTS solutions were again kept for stirring at room temperature to further reduce the particle size. Finally, these solutions were separated into three-three separate parts (~5 ml each) in small bottles; in one part of solution, added a few drops (~10 drops) of polyvinyl alcohol (PVA), another part of solution mixed with a few drops (~10 drops) dimethyl sulfoxide (DMSO), and the third part remained as it is for both CZTS and CZGTS. To get appropriate forms of the solutions for the doctor blade coating, all six (both CZTS and CZGTS) samples were kept for 5-10 min ultrasonication. It was ensured to keep almost same thickness in between the SLG glass substrate and coating knife for the doctor blade-coated thin films. The prepared sulfurized (at 550°C, ~40 min) thin film structural characterization were performed from the X-ray diffractometer, field effect scanning microscopy (FESEM), energy dispersive spectroscopy (EDS), Raman spectroscopy, and UV/visible spectroscopy.

3. Results and Discussion

Synthesized CZTS and CZGTS (Figure 1(i)) and their DMSO and PVA mixed solutions doctor blade-coated (Figure 1(ii)) thin films on SLG substrate are exhibited in Figure 1 (iii (a–f)). By the appearance, this ~550°C sulfurized thin film colour seems quite distinct to each other. Appearance of the distinct colour surfaces can be directly correlated to rather distinct crystal growths such as grain sizes and porosity, under the identical sulfurization condition. Further, these thin film thickness profiles are given in Figures 2(a)–2(f). It gives these doctor blade-coated thin film thickness lies in between ~1.5 and ≤2.5 μm. The obtained thickness value of the thin films lies in range of an optimum active layer thickness for multilayer chalcogen rich solar cell devices.

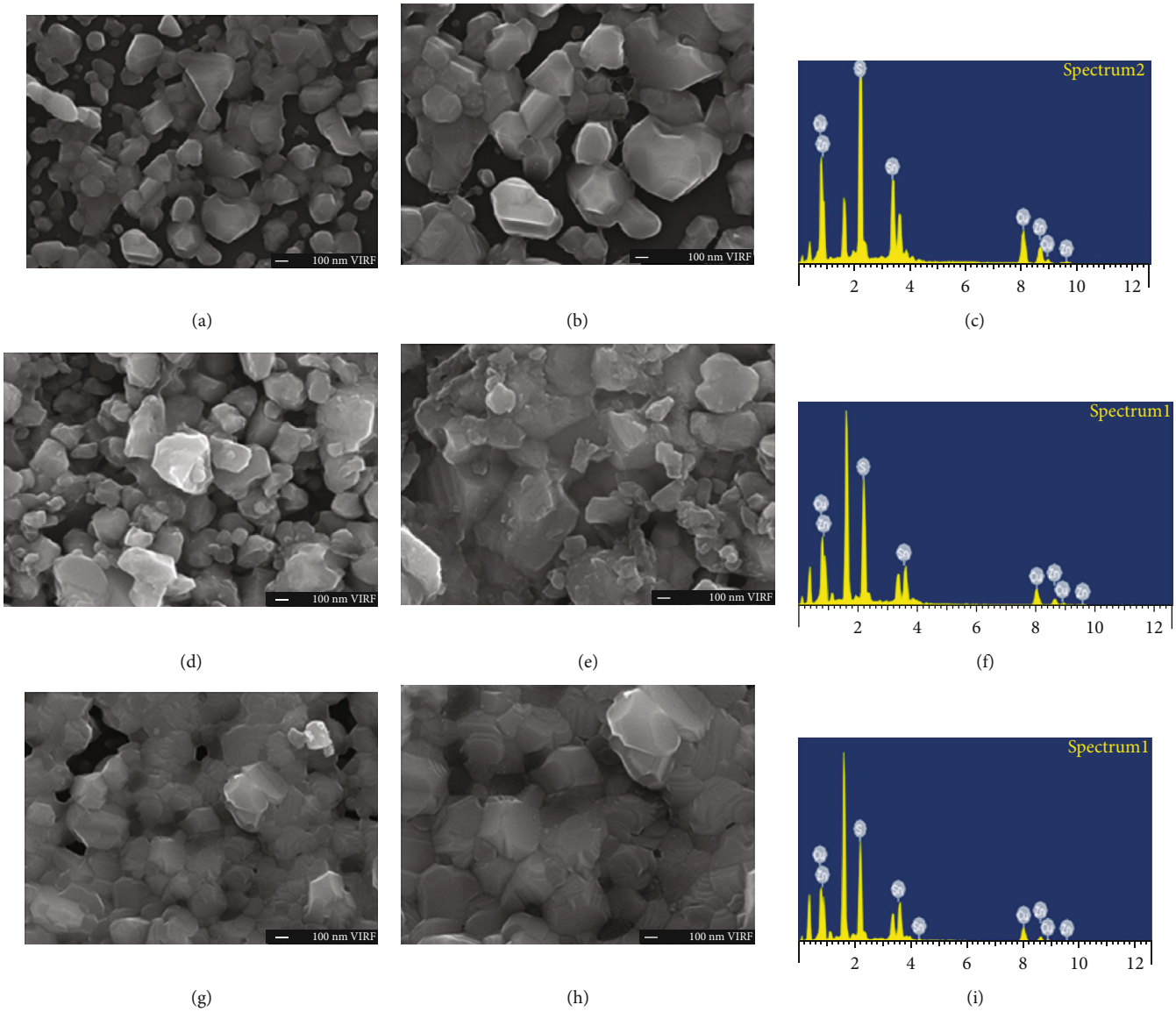

Figure 3: (a–i). FE-SEM and EDS patterns for the CZTS, CZTS-PVA, and CZTS-DMSO thin films.

To realize different binder solvent impact on developed thin film grain sizes and porosity, we have performed the field effect scanning microscopy (FESEM) measurement. Figures 3(a)–3(i) represents surface morphologies at different scale with the EDS patterns for the CZTS and DMSO, and PVA mixed thin films. The parent CZTS thin film surface morphology reveals slightly smaller grains and inferior grain connectivity to each other (see Figures 3(a) and 3(b)). However, PVA containing thin film grain connectivity seems to be compact (see Figures 3(d) and 3(e)), while the DMSO containing thin film grain exhibits a clear distinction in term of larger grain sizes with the enhanced connectivity (see Figures 3(g) and 3(h)). The elemental concentration in these thin films is obtained as per designed alloying compositional ratio, as depicted in Figures 3(c), 3(f), and 3(i). The obtained elemental compositional ratio empirical values are listed in Table 1. Moreover, Figures 4(a)–4(i) is representing FESEM surface morphologies and EDS patterns for the Ge-alloyed CZTS thin films. The Ge-alloyed CZTS thin film exhibits (see Figures 4(a) and 4(b)) a wide difference in grain size compared to non-Ge-alloyed thin films. Besides, a large size grain growth CZGTS thin film has inferior grain connectivity compared to CZGTS-PVA thin film (see Figures 4(d) and 4(e)), though reduction in crystal grain sizes has appeared for the CZGTS-PVA thin film. Further, the DMSO containing CZGTS thin film (see Figures 4(g) and 4(h)) is exhibited slightly improved grain growth morphology compared to CZGTS-PVA having superior crystal grain boundaries. The alloying elemental concentrations in CZGTS-based thin films has also obtained as per designed alloying compositional ratio, as depicted in Figures 4(c), 4(f), and 4(i). The obtained empirical elemental compositional ratio amounts are given in Table 2.

Such variation in crystallite grain sizes and their boundaries due to incorporation of PVA and DMSO in CZTS and CZGTS may affect the crystallographic structures of the materials. To examine this, we have performed the XRD

Table 1: EDS analysis obtained alloying element average concentration for the CZTS, CZTS-PVA, and CZTS-DMSO doctor-coated thin films.

CZTS		CZTS-PVA		CZTS-DMSO	
Element	Atomic%	Element	Atomic%	Element	Atomic%
S	50.52	S	50.94	S	51.64
Cu	19.94	Cu	15.77	Cu	18.77
Zn	12.54	Zn	15.05	Zn	12.90
Sn	16.99	Sn	18.24	Sn	16.69
Total:	100.00	Total:	100.00	Total:	100.00

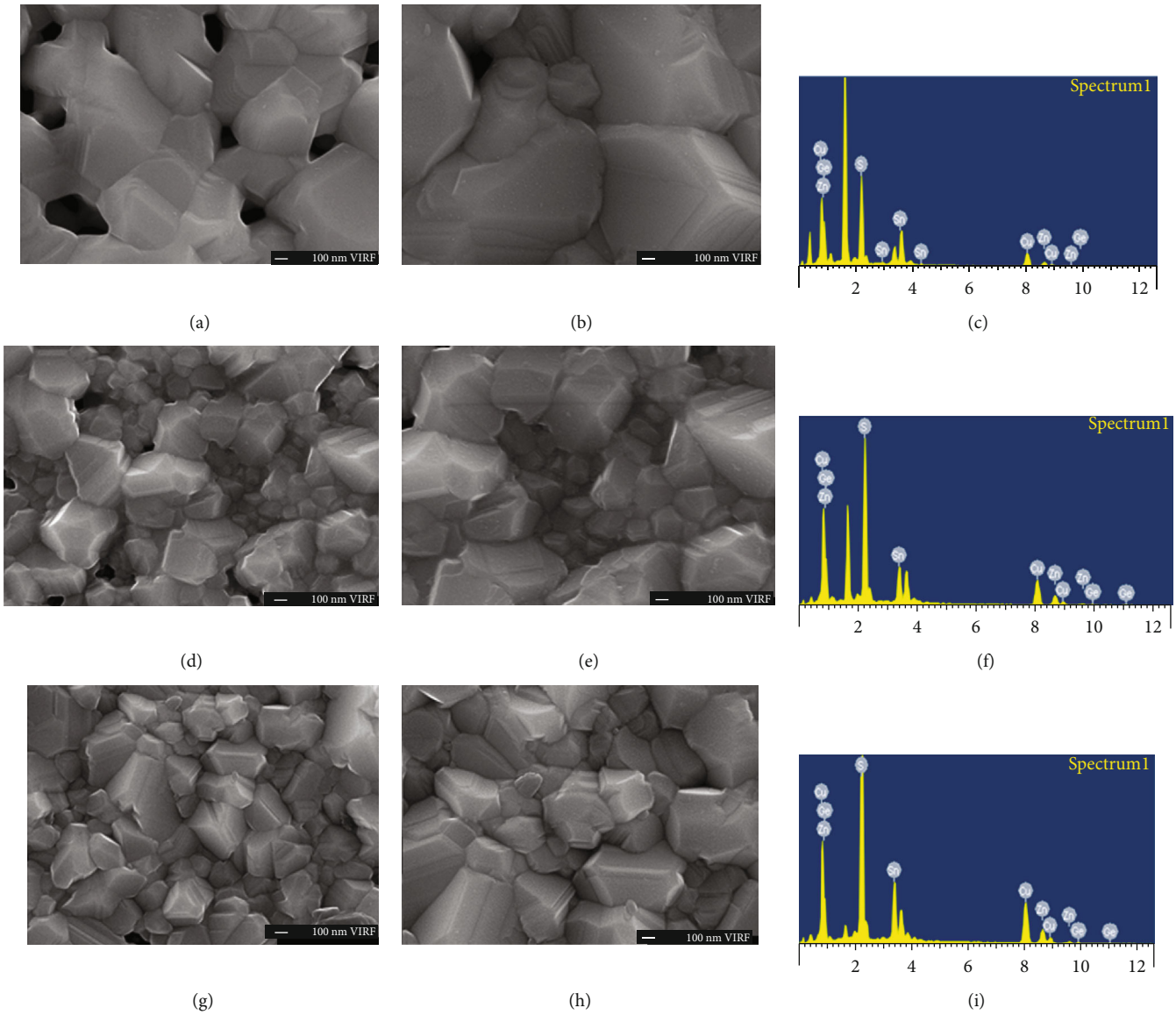

Figure 4: (a–i) FE-SEM and EDS patterns for the CZGTS, CZGTS-PVA, and CZGTS-DMSO thin films.

measurement for the fabricated thin films, as illustrated in Figure 5. All six thin films exhibited the prime CZTS strong crystallographic peak corresponding to (112) plane at 2θ value 28°, along with other week CZTS characteristic peaks at 2θ values 16°, 18°, 33°, 47°, and 56°, corresponding to crystallographic planes (002), (101), (200), (220), and (311). The week crystallographic (002) peak is suppressed sufficiently/or almost disappear in Ge-alloyed CZTS thin films, while the (220) and (311) crystallographic plane peaks are slight shift toward the higher angle side for the CZGTS, CZGTS-PVA,

Table 2: EDS analysis obtained alloying element average concentration for the CZGTS, CZGTS-PVA, and CZGTS-DMSO doctor-coated thin films.

CZGTS		CZGTS-PVA		CZGTS-DMSO	
Element	Atomic%	Element	Atomic%	Element	Atomic%
S	52.90	S	53.49	S	53.49
Cu	22.26	Cu	23.16	Cu	23.16
Zn	8.97	Zn	9.97	Zn	9.97
Ge	2.26	Ge	2.71	Ge	2.71
Sn	13.61	Sn	10.67	Sn	10.67
Total:	100.00	Total:	100.00	Total:	100.00

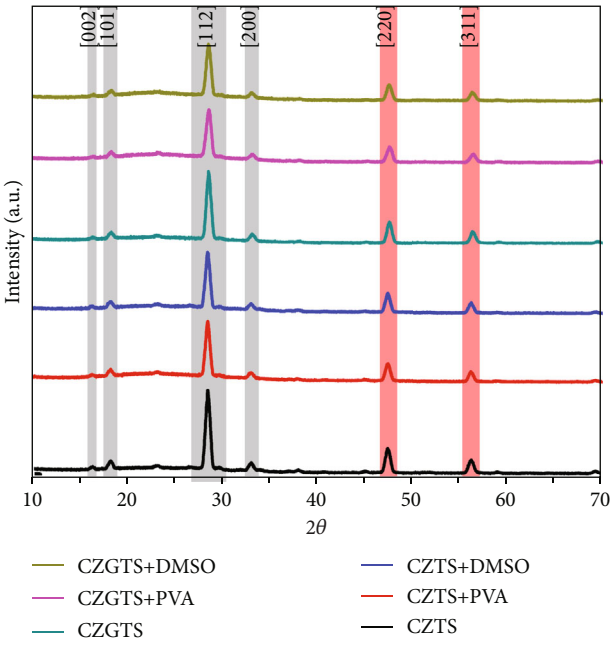

Figure 5: XRD patterns for the CZTS, CZTS-PVA, CZTS-DMSO, CZGTS, CZGTS-PVA, and CZGTS-DMSO thin films.

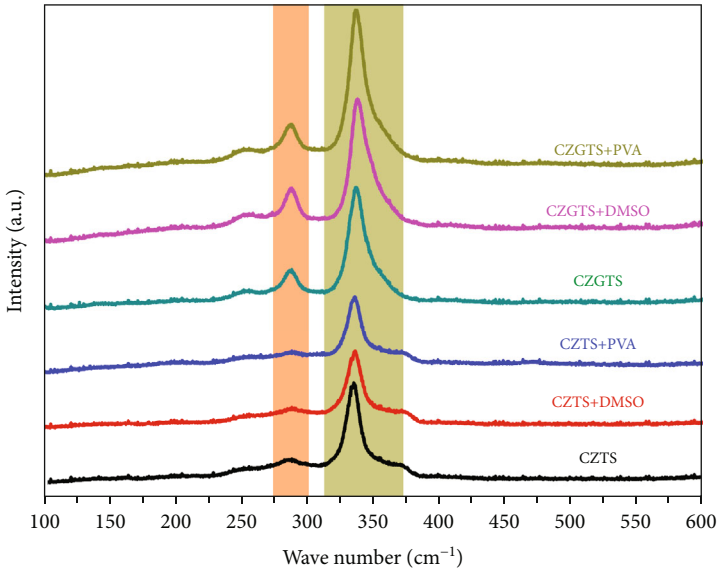

Figure 6: Raman spectrum for the CZTS, CZTS-DMSO, CZTS-PVA, CZGTS, CZGTS-DMSO, and CZGTS-PVA thin films.

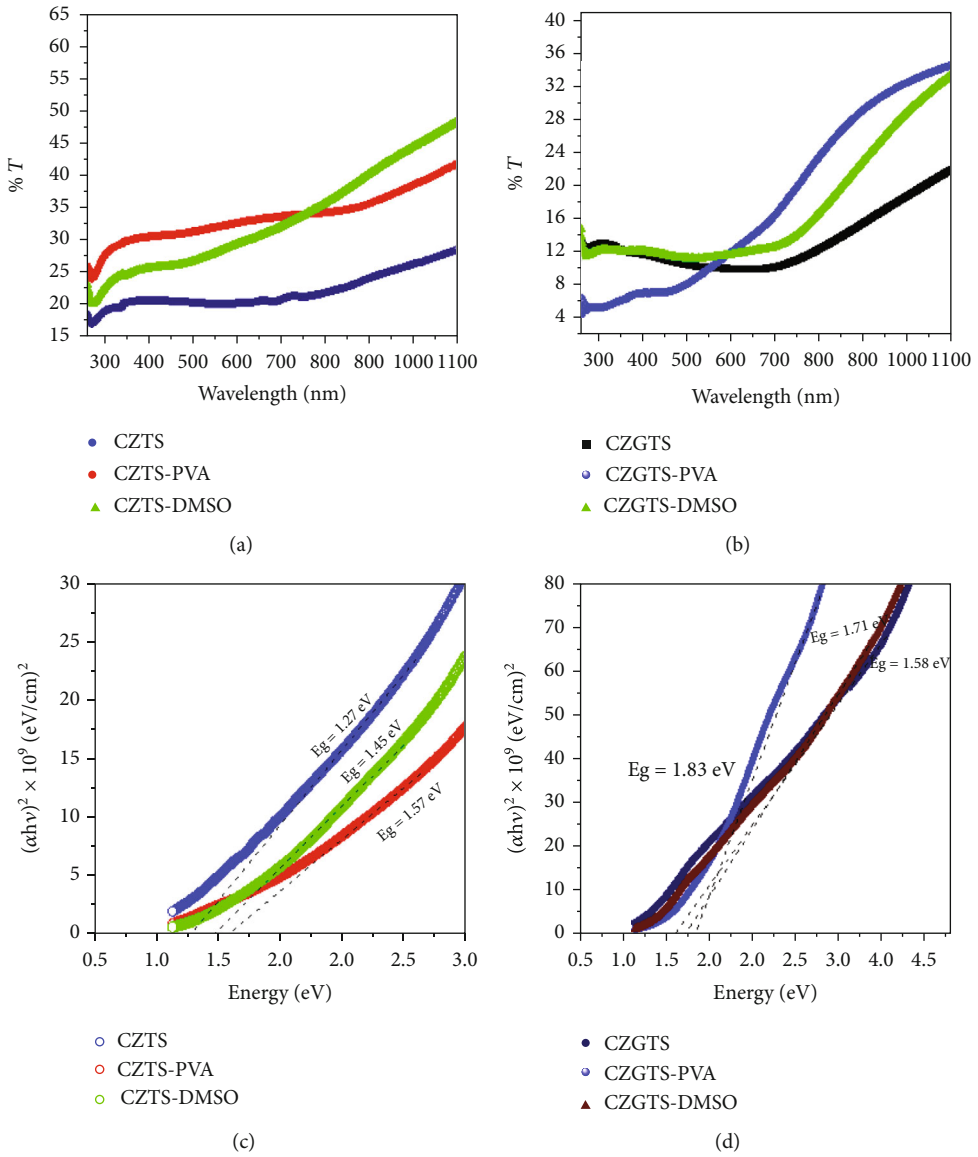

Figure 7: (a–d) UV/visible transmission and Tauc plots for the CZTS, CZTS-PVA, and CZTS-DMSO and CZGTS, CZGTS-PVA, and CZGTS-DMSO thin films.

and CZGTS-DMSO thin films. This can be correlated to crystallographic changes in CZTS due to incorporation of semimetallic Ge. This crystallographic variation can also be evident from the Raman measurement result. The prime Raman kesterite phase broad peak vibration in the wave number range 314 to 370 cm^{-1} is observed, as depicted in Figure 6 [17, 18]. The strongest "A" mode peak position is obtained around the 338 cm^{-1}. A distinguishable Raman peak shift toward the higher wave number is appeared for the CZTS, CZTS-DMSO, CZTS-PVA, CZGTS, CZGTS-DMSO, and CZGTS-PVA thin films. Along with a weak peak toward the lower wave number (275 to 300 cm^{-1}) is also noticed for the Ge containing thin films. The gradual Raman peak shift and appearance of addition weak peak in CZGTS thin films indicates atomic distribution of the materials affected with the incorporation of different solvent as well as semimetallic Ge.

The uv/visible optical property of the active layer material in a multilayers photovoltaic solar cell is an important parameter, because incident external solar light induced charge carrier generation in this layer, which depends on material light absorption ability. The recorded uv/visible transmission spectrum of the CZTS, CZGTS, and PVA, DMSO containing thin films is given in Figures 7(a) and 7(b). Using the obtained UV/visible transmission spectrums, we have evaluated the optical energy band gaps for these thin films by employing the well know Tauc relationship [19]. Both CZTS and CZGTS thin films are exhibiting a considerable optical energy band gap increment with the addition of PVA and DMSO, as illustrated in Figures 7(c) and 7(d). The obtained optical energy band gaps for the CZTS, CZTS-DMSO, and CZTS-PVA and CZGTS, CZGTS-DMSO, and CZGTS-PVA are 1.27, 1.45, and 1.57 and 1.58, 1.71, and 1.83 eV, respectively. Change in optical energy

band gaps of CZTS and CZGTS due to incorporation of PVA and DMSO could be correlated to formation of a few additional subenergy levels within the complex configuration under influence of the different reactivity during fabrication process.

Hence, the physical property variation in CZTS owing to incorporation of semimetallic element Ge under different binder solvent effect could correlate to change in their antisite trap charges [5, 14]. CZTS can have two dominant antisite charge trapping with the Cu and Zn energies 20 meV and 120 meV [20]. These two element energies can be considered in deeper trapping range, while a significant difference in between bonding energies of Ge and Sn can also contribute substantially with the increasing trap energy. Predominantly, Ge containing sites can lie in deeper traps. The Ge deeper traps (106–170 meV) can be close to Fermi level and may not be fully ionized even at room temperature [5, 14, 21–24]. As consequence, structural and optoelectronics changes might be appeared in Ge-alloyed CZTS [5, 14, 21–24]. Significantly, the CZTS legend share bonds exposing ability of the binder solvents PVA and DMSO may also be contributed substantially. Therefore, a gradual change has appeared in grain sizes, XRD, Raman peaks, and optical energy band gaps.

4. Conclusions

In the conclusive remarks, authors have discussed the low cost, easy, nontoxic photovoltaic CZTS material synthesis route with the impact of the additional small amount of the Ge in CZTS system. Among this, also demonstrated the physical property variation due to addition of small amounts of the PVA and DMSO in CZTS and CZGTS materials. Experimental evidences have revealed doctor-coated sulfurized thin film thickness is in well-define range of multilayer inorganic solar cells. The grain sizes and compactness of the surface morphologies of the CZTS and PAV and DMSO have been noticed in rather improved sequence. While incorporation of element Ge gives the larger grains with rough porosity quality, amounts of PVA and DMSO have slightly reduced the grain sizes with improved compactness. Incorporation of Ge and PVA and DMSO also impacted the parent material crystallographic structure that have been reflected in terms of slight shift in XRD peak positions for high 2θ (47 and 56) values. A consistence Raman prime peak shift with the appearance of additional week peak in Ge containing materials has also correlated to structural changes in CZTS and CZGTS due to incorporation of PVA and DMSO contents in parent configurations. The uv/visible optical property have also been affected due to incorporation of Ge in CZTS as well PVA and DMSO; their obtained energy band gaps are 1.27, 1.45, and 1.57 and 1.58, 1.71, and 1.83 eV, respectively. Hence, this study leads DMSO containing film can be more appropriate than others to fabricate multilayer PV devices.

Data Availability

The data used to support the findings of this study are available from the corresponding author upon request.

Conflicts of Interest

Herein, the authors declare that they have no conflicts of interest.

Acknowledgments

AKS is thankful to the University of Johannesburg, Department of Mechanical Engineering Science (APK), Faculty of Engineering and the Built Environment (FEBE), for the support under the PDRF program. Also, the authors are thankful to Incheon National University (INU), Incheon, South Korea. Prof Jen would like to thank the support from URC and NRF South Africa. Authors AKS and MS are thankful to the Deanship of Scientific Research at King Khalid University, Abha, Saudi Arabia, for providing support under grant no. R.G.P.1/102/42.

References

[1] X. Song, X. Ji, M. Li, W. Lin, X. Luo, and H. Zhang, "A review on development prospect of CZTS based thin film solar cells," *International Journal of Photoenergy*, vol. 2014, Article ID 613173, 11 pages, 2014.

[2] M. Ravindiran and C. Praveenkumar, "Status review and the future prospects of CZTS based solar cell – a novel approach on the device structure and material modeling for CZTS based photovoltaic device," *Renewable and Sustainable Energy Reviews*, vol. 94, pp. 317–329, 2018.

[3] H. Zhou, W. C. Hsu, H. S. Duan et al., "CZTS nanocrystals: a promising approach for next generation thin film photovoltaics," *Energy & Environmental Science*, vol. 6, no. 10, pp. 2822–2838, 2013.

[4] M. Benchikri, O. Zaberca, R. El Ouatib et al., "A high temperature route to the formation of highly pure quaternary chalcogenide particles," *Materials Letters*, vol. 68, pp. 340–343, 2012.

[5] D. Huang and C. Persson, "Band gap change induced by defect complexes in Cu_2ZnSnS_4," *Thin Solid Films*, vol. 535, pp. 265–269, 2013.

[6] A. Wangperawong, J. S. King, S. M. Herron, B. P. Tran, K. Pangan-Okimoto, and S. F. Bent, "Aqueous bath process for deposition of Cu2ZnSnS4 photovoltaic absorbers," *Thin Solid Films*, vol. 519, no. 8, pp. 2488–2492, 2011.

[7] K. Tanaka, Y. Fukui, N. Moritake, and H. Uchiki, "Chemical composition dependence of morphological and optical properties of Cu2ZnSnS4 thin films deposited by sol–gel sulfurization and Cu2ZnSnS4 thin film solar cell efficiency," *Solar Energy Materials & Solar Cells*, vol. 95, no. 3, pp. 838–842, 2011.

[8] J. Zhong, Z. Xia, C. Zhang et al., "One-pot synthesis of self-stabilized aqueous nanoinks for Cu2ZnSn(S,Se)4 solar cells," *Chemistry of Materials*, vol. 26, no. 11, pp. 3573–3578, 2014.

[9] D. B. Khadka, S. Y. Kim, and J. H. Kim, "Ge-alloyed CZTSe thin film solar cell using molecular precursor adopting spray pyrolysis approach," *RSC Advances*, vol. 6, no. 44, pp. 37621–37627, 2016.

[10] N. Saini, J. K. Larsen, K. V. Sopiha, J. Keller, N. Ross, and C. P. Björkman, "Germanium incorporation in Cu_2ZnSnS_4 and formation of a Sn–Ge gradient," *Physica Status Solidi (a)*, vol. 216, article 1900492, 2019.

[11] W. Shockley and H. J. Queisser, "Detailed balance limit of efficiency of p-nJunction solar cells," *Journal of applied physics*, vol. 32, no. 3, pp. 510–519, 1961.

[12] J. Chen, F. Wang, B. Yang et al., "Fabrication of Cu2ZnSnS4 thin films based on facile nanocrystals-printing approach with rapid thermal annealing (RTA) process," *Coatings*, vol. 9, no. 2, p. 130, 2019.

[13] M. Jiang and X. Yan, "Cu_2ZnSnS_4 thin film solar cells: present status and future prospects," in *INTECH book "Solar Cells-Research and Application Perspectives", Chapter-5*, 2013.

[14] J. Moore, C. Hages, M. Lundstrom, and R. Agrawa, "Influence of Ge doping on defect distributions of Cu_2Zn (Sn_x Ge_{l-x}) (S_y Se_{l-y}) fabricated by nanocrystal ink deposition with selenization," in *2012 38th IEEE Photovoltaic Specialists Conference*, pp. 001475–001480, Austin, TX, USA, 2012.

[15] G. M. Ford, Q. Guo, R. Agrawal, and H. Hillhouse, "Earth abundant element Cu2Zn(Sn1−xGex)S4 nanocrystals for tunable band gap solar cells: 6.8% efficient device fabrication," *Chemistry of Materials*, vol. 23, no. 10, pp. 2626–2629, 2011.

[16] A. Lafond, L. Choubrac, C. G. Deudon, P. Deniard, and S. Jobic, "Crystal structures of photovoltaic chalcogenides, an intricate puzzle to solve: the cases of CIGSe and CZTS materials," *Zeitschrift für Anorganische und Allgemeine Chemie*, vol. 638, no. 15, pp. 2571–2577, 2012.

[17] P. K. Sarswat, M. L. Free, and A. Tiwari, "Temperature-dependent study of the Raman a mode of Cu2ZnSnS4 thin films," *Physica Status Solidi B: Basic Solid State Physics*, vol. 248, no. 9, pp. 2170–2174, 2011.

[18] D. Dumcenco and Y. S. Huang, "The vibrational properties study of kesterite Cu2ZnSnS4 single crystals by using polarization dependent Raman spectroscopy," *Optical Materials*, vol. 35, no. 3, pp. 419–425, 2013.

[19] M. Ben Rabeh, R. Touatti, and M. Kanzari, "Structural and optical properties of the new absorber Cu_2ZnSnS_4 thin films grown by vacuum evaporation method," *International Journal of Engineering Practical Research*, vol. 2, pp. 71–75, 2013.

[20] J. Li, D. Wang, X. Li, Y. Zeng, and Y. Zhang, "Cation substitution in earth-abundant kesterite photovoltaic materials," *Advancement of Science*, vol. 5, article 1700744, 2018.

[21] L. Sun, H. Shen, H. Huang, A. Raza, Q. Zhao, and J. Yang, "Influence of Ge layer location on performance of flexible CZTSSe thin film solar cell," *Vacuum*, vol. 165, pp. 186–192, 2019.

[22] Q. Guo, G. M. Ford, W. C. Yang, C. J. Hages, H. W. Hillhouse, and R. Agrawal, "Enhancing the performance of CZTSSe solar cells with Ge alloying," *Solar Energy Materials & Solar Cells*, vol. 105, pp. 132–136, 2012.

[23] S. Giraldo, E. Saucedo, M. Neuschitzer et al., "How small amounts of Ge modify the formation pathways and crystallization of kesterites," *Energy & Environmental Science*, vol. 11, no. 3, pp. 582–593, 2018.

[24] D. B. Khadka, S. Y. Kim, and J. H. Kim, "Effects of Ge alloying on device characteristics of kesterite-based CZTS Se thin film solar cells," *Journal of Physical Chemistry C*, vol. 120, no. 8, pp. 4251–4258, 2016.